Optical Physical-Layer Network Coding

Zhixin Liu, Ming Li, Lu Lu, Chun-Kit Chan, Soung-Chang Liew, and Lian-Kuan Chen

***Abstract*— The application of physical-layer network coding (PNC) in optical communications is explored. We propose and demonstrate a practical optical PNC prototype for multicast protection in optical flow, burst, and packet switching networks. Different from conventional theoretical PNC studies, our proposed optical PNC system does not require bit synchronization and can be easily implemented.**

***Index Terms*— Fiber protection, multicast network, physical-layer network coding (PNC), polarization multiplexing.**

I. Introduction

DRIVEN by the recent popularity of high-definition videos and data-intensive applications, a steady increase of data traffic in optical networks by 40% every year has been witnessed [1]. In order to realize more flexible switching granularity in high-capacity wavelength-routed networks, several robust optical transport schemes, including optical flow switching (OFS), optical burst switching (OBS) and optical packet switching (OPS), have been widely investigated. Recently, network coding [2] has also aroused a lot of attention for its potential to enhance the throughput and robustness of multicast networks [3], [4]. It could be realized by performing linear operations, such as logic exclusive-OR (XOR), on two signals at the network layer so as to share the same network link, thus reduces the required network resources.

To enhance system efficiency, it is more preferable to realize network coding in the physical layer. All-optical XOR gates could be utilized to realize physical-layer network coding (PNC) [5] in optical layer, however, the required nonlinear optical signal processing techniques as well as the stringent optical signal synchronization hinder the practicality of the implementation. Fortunately, PNC is not limited to techniques based on logical operation. It can also been realized by adding up the two signal frames, as demonstrated in wireless communications [6]. One of the key issues in PNC is how to assure the asynchrony between the signals transmitted by different transmitters [7]. It has been shown that the asynchrony penalty is small, provided that proper decoding method is adopted. Recently, analog network coding (ANC) [8], which does not require bit synchronization and can be decoded incoherently, has also been proposed.

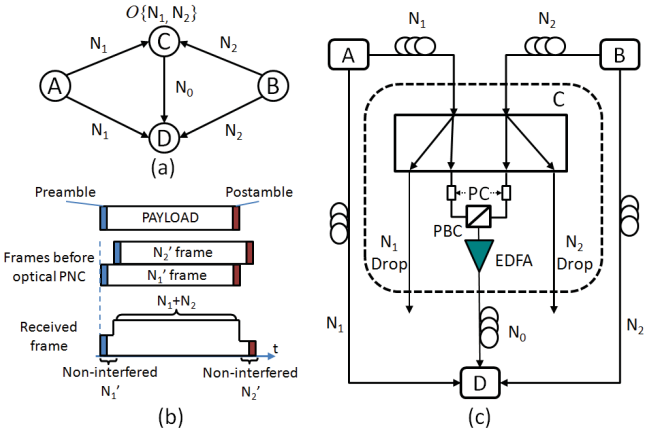

Fig. 1. (a) Example network utilizing network coding. (b) Frames before and after network coding. (c) Proposed optical PNC implementation.

Motivated by ANC, we propose optical PNC as the first implementation of PNC in optical networks. Two transmitted optical signal frames are polarization-multiplexed to form the network-coded frame, which is then incoherently detected by a single photo-detector (PD) at the receiver. Signal decoding is realized by subtracting the reconstructed waveform of either one of the two optical signal frames from that of the received network-coded frame. We further experimentally demonstrate the feasibility of the scheme with 10-Gb/s non-return-to-zero on-off keying (NRZ-OOK) optical frames.

II. Multicast Protection via Network Coding

Consider a four-node network, as shown in Fig. 1(a), A (node A) and B (node B) simultaneously transmit their respective multicast frames, N_1 and N_2, to both C (node C) and D (node D). The traditional way to protect single link failure (e.g. A-D) is to set up a connection between C and D, which relays N_1 from C to D. However, this incurs a certain setup time, which is undesirable when the data is very sensitive to network delay. To protect links A-D and B-D against any single link failure, C needs to relay both N_1 and N_2 to D on link C-D. By applying network coding, if N_1 and N_2 overlap in time domain, C only needs to forward a function $N_0 = O\{N_1, N_2\}$ to D. Here, $O\{N_1, N_2\}$ can be any function which has the property that N_2 can be derived from N_1 and N_0 in case of failure in link B-D only, while N_1 can be derived from N_2 and N_0 in case of failure in link A-D only. As a result, the network resources for single link failure protection are saved.

Manuscript received April 5, 2012; revised June 11, 2012; accepted June 12, 2012. Date of publication July 6, 2012; date of current version July 31, 2012. This work was supported in part by the AoE Grant E-02/08, in part by the General Research Funds Project 414911 under the University Grant Committee of the Hong Kong Special Administrative Region, China, in part by the CUHK Direct Grant 2050464, and in part by the China 973 Program under Project 2012CB315904.

The authors are with the Department of Information Engineering, Chinese University of Hong Kong, Shatin, Hong Kong (e-mail: lzx009@ie.cuhk.edu.hk; ckchan@ie.cuhk.edu.hk).

Color versions of one or more of the figures in this letter are available online at http://ieeexplore.ieee.org.

Digital Object Identifier 10.1109/LPT.2012.2204972

III. Proposed Optical PNC Scheme

Fig. 1(b) shows the structures of the optical frames before and after network coding. Each frame comprises both preamble and postamble, which are unique for each source node and the lengths of the two input frames are assumed to be equal. The waveform of N_0 generated through optical PNC is the addition of the waveforms of N_1' and N_2' (i.e. the respective replicas of N_1 and N_2) with certain time shift between them, such that the leading and the trailing portions of N_0 are free of signal interference. Frame-level scheduling is needed to assure this.

IV. Proposed Optical PNC Scheme

To illustrate the process of network decoding, it is assumed that the bit sequence of N_1 is known and the bit sequence of N_2 is to be decoded from N_0. From the interference-free preamble and postamble in N_0, it can be determined whether N_1' or N_2' comes earlier in time domain. Without loss of generality, here we assume that N_1' comes earlier. With the interference-free preamble of N_1' extracted from N_0, the precise timing and amplitude information of N_1 component contained in N_0 can be determined. Together with the known bit sequence of N_1, the waveform of N_1' can be reconstructed, which is then subtracted from N_0. The resultant signal is basically the N_2' component contained in N_0, and it is then used to derive the bit sequence of N_2. The impulse response of the system, which is utilized for reconstructing N_1', can be measured in advance or estimated from the interference-free preamble. For network decoding, both the waveforms of the received network-coded frame and the bit sequence of the successfully received frame need to be stored in the receiver.

Fig. 1(c) shows the system architecture of the proposed optical PNC scheme for an optical network, whose topology is the same as that in Fig. 1(a). At node C, a copy of input frame N_1 from node A and a copy of input frame N_2 from node B are combined, via a polarization beam combiner (PBC), which multiplexes N_1 and N_2 on two orthogonal polarizations. Thus, the network-coded frame N_0 is generated. Polarization controllers (PCs) are used to adjust the polarizations of the input frames so that the insertion loss at PBC can be minimized. The insertion loss at PBC can be monitored by measuring the output optical signal power at the other output port of the PBC. Time shifting between the frames is realized by proper scheduling in the network layer. The network-coded signal N_0 is then amplified by an erbium-doped fiber amplifier (EDFA) before being relayed to node D, where the network-coded signal is detected by a single PD and the missing frame can be recovered, when necessary.

V. Experimental Results and Discussion

The experimental setup is depicted in Fig. 2. The output of a distributed feedback laser diode (DFB-LD) was modulated with a Mach–Zehnder modulator (MZM) driven by a periodic binary pattern at 10 Gb/s. Each period of the binary pattern consisted of a frame of 131583 bits followed by 2×10^5 zero bits. Each frame contained repeated $2^{17} - 1$ pseudorandom bit sequence (PRBS) as payload, to which two 256-bit Gold

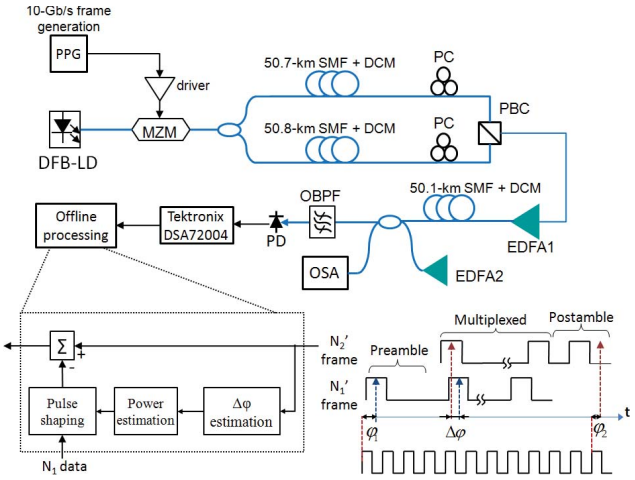

Fig. 2. Experimental setup.

sequences were added, one at the beginning and the other at the end, as preamble and postamble, respectively. The output NRZ-OOK signal was then split into two branches to emulate the transmission of frame N_1 and frame N_2 in different paths. The two fiber branches consisted of 50.7-km and 50.8-km standard single-mode fiber (SSMF) segments which had ~17 ps/(nm·km) chromatic dispersion coefficient at 1552.13 nm, followed by dispersion compensation module (DCM) of −680 ps/nm chromatic dispersion, respectively. The polarizations of the transmitted frames, N_1 and N_2, were controlled by two PCs before being orthogonally multiplexed via a PBC to generate the network-coded frame N_0. The generated frame N_0 was then amplified by EDFA1, before being transmitted over another 50.1-km SSMF span, whose chromatic dispersion was also compensated with a DCM. On the receiver side the optical signal-to-noise ratio (OSNR) of the optical signal was adjusted, via injection of amplified spontaneous emission (ASE) noise from EDFA2. The optical signal was then filtered by a 0.8-nm optical bandpass filter (OBPF) to remove out-of-band ASE noise. Finally the filtered optical signal was detected by a single PIN photodiode and sampled at 50 GS/s by a Tektronix DSA72004 digital serial analyzer (DSA). Network decoding was implemented by off-line digital signal processing.

As shown in Fig. 2, since the preamble was interference-free, φ_1(sampling phase for N_1' with respect to the reference clock) was able to be estimated from the preamble by selecting φ_1 that gave the highest Q-factor. With the same criteria, φ_2(sampling phase for N_2') was estimated from the postamble. The difference of the sampling phases could then be calculated by $\Delta\varphi = \varphi_1 - \varphi_2$. In addition, both the power and the pulse shape of N_1' in N_0 were able to be estimated from the preamble. With all these extracted information as well as the decided bit sequence of N_1, an estimation of N_1' in N_0 was able to be constructed. Therefore, N_2' was able to be recovered by subtracting the estimated N_1' from N_0, and then the bit sequence of N_2 could be decided. Note that the clock frequency of N_1' was exactly the same as that of N_1 and with some additional digital signal processing, the proposed optical PNC scheme also worked even when the clock frequencies of

N_1 and N_2 were not equal or the clock frequencies drifted with time.

Fig. 3 shows the waveform of the received network-coded frame N_0. The misalignment between the frames N_1' and N_2' was around 0.58 μs, which corresponded to about 5800 bits. Clear NRZ-OOK eye was observed in the interference-free starting and ending parts of N_0. The middle part showed four levels corresponding to the four possible combinations of N_1' and N_2'.

Fig. 4 shows the measured as well as the simulated bit-error rate (BER) curves for N_1 and N_2 frames without and with our proposed network coding/decoding scheme. For both the cases without and with optical PNC, the optical signal was directly detected by a single PD without polarization filtering. The BER was averaged over 13 frames, which corresponded to a total of more than 1.7×10^6 bits. The powers of N_1' and N_2' in N_0 were kept to be the same level and the bits of N_1' and N_2' were aligned in the simulations. However, in the experiment such precise control of N_1' and N_2' could hardly be achieved, which also contributed to the discrepancy between the simulation and experimental results. The OSNR penalty (BER $= 10^{-3}$) induced by network coding/decoding in the simulation was 7.8 dB, and those in the experimental results for N_1, and N_2 were 7.3 dB and 8.3 dB, respectively.

The OSNR penalty was mainly induced by the beat noise between the optical signal and the ASE noise. At sampling time the generated photo-current for N_2 without network coding/decoding is

$$\begin{aligned} i_2 &= R\left(|s_2+n_x|^2+|n_y|^2\right) \\ &= R\left(s_2^2+2s_2n_{xc}+n_{xc}^2+n_{xs}^2+n_{yc}^2+n_{ys}^2\right) \end{aligned} \quad (1)$$

in which R was the responsivity of the PD, s_2 was the amplitude of N_2, $n_x = n_{xc}+jn_{xs}$ and $n_y = n_{yc}+jn_{ys}$ were the amplitudes of the two polarizations of the ASE noises within the receiver bandwidth. We assumed that the powers of n_x and n_y were both σ^2, and s_2 was A_2 for bit '1' and 0 for bit '0', then the Q-factor of N_2 at sampling time:

$$\begin{aligned} Q_2 &= \frac{E(i_2|s_2=A_2)-E(i_2|s_2=0)}{\sqrt{Var(i_2|s_2=A_2)}+\sqrt{Var(i_2|s_2=0)}} \\ &= \frac{R(A_2^2+2\sigma^2)-R(2\sigma^2)}{\sqrt{R^2(2A_2^2\sigma^2+2\sigma^4)}+\sqrt{R^2(2\sigma^4)}} \\ &= \frac{A_2^2/\sigma^2}{\sqrt{2A_2^2/\sigma^2+2}+\sqrt{2}} \end{aligned} \quad (2)$$

and the corresponding BER

$$BER = \frac{1}{2}erfc\left(\frac{Q_2}{\sqrt{2}}\right) \quad (3)$$

in which $erfc(\bullet)$ was the complement error function.

Similarly, after network decoding the generated photo-current for N_2' at sampling time was

$$\begin{aligned} i_2' &= R\left(|s_2+n_x|^2+|s_1+n_y|^2\right)-Rs_1^2 \\ &= R\left(s_2^2+2s_2n_{xc}+n_{xc}^2+n_{xs}^2+2s_1n_{yc}+n_{yc}^2+n_{ys}^2\right) \end{aligned} \quad (4)$$

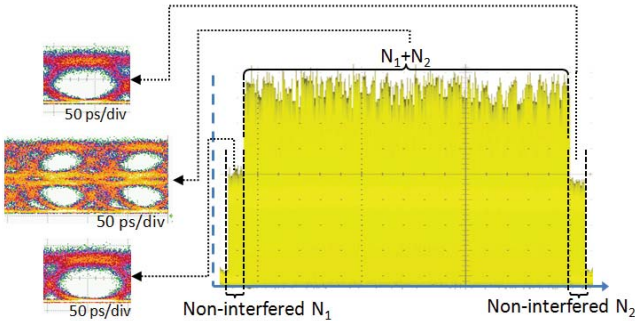

Fig. 3. Waveform and eye diagrams of the received frame N_0.

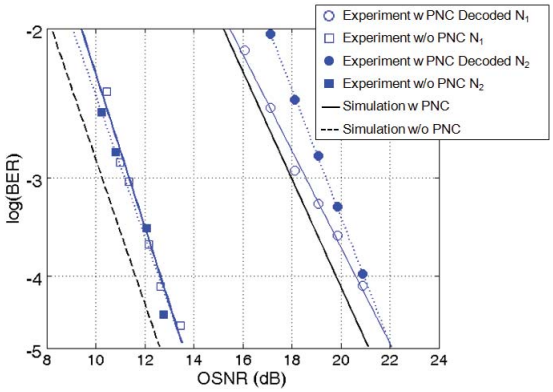

Fig. 4. BER performance of N_1 and N_2 without and with network coding and decoding. Points are fitted with straight line.

in which s_1 was the amplitude of N_1' at the sampling time, and R was the responsivity of the PD. Assuming that s_1 and s_2 were independent, after some algebra at the sampling time, the corresponding Q-factor of N_2' when $s_1 = A_1$

$$\begin{aligned} &Q_2'|_{s_1=A_1} \\ &= \frac{E(i_2'|s_2=A_2,s_1=A_1)-E(i_2'|s_2=0,s_1=A_1)}{\sqrt{Var(i_2'|s_2=A_2,s_1=A_1)}+\sqrt{Var(i_2'|s_2=0,s_1=A_1)}} \\ &= \frac{R(A_2^2+2\sigma^2)-R(2\sigma^2)}{\sqrt{R^2(2A_2^2\sigma^2+2A_1^2\sigma^2+2\sigma^4)}+\sqrt{R^2(2A_1^2\sigma^2+2\sigma^4)}} \\ &= \frac{A_2^2/\sigma^2}{\sqrt{2A_2^2/\sigma^2+2A_1^2/\sigma^2+2}+\sqrt{2A_1^2/\sigma^2+2}} \end{aligned} \quad (5)$$

and the corresponding BER

$$BER' = E\left[\frac{1}{2}erfc\left(\frac{Q_2'|_{s_1=A_1}}{\sqrt{2}}\right)\right] \quad (6)$$

in which $E[\bullet]$ was the expectation over all possible values of A_1, the amplitude of N_1' at the sampling time of N_2'. Note that since N_1 and N_2 did not need to be aligned when the network coding was performed, A_1 could take more than two values.

Comparing (1) and (4), it could be concluded that network coding/decoding introduced a noise term $2s_1n_{yc}$, which degraded the BER. When the bits of N_1' and N_2' were perfectly aligned and their amplitudes were both A, s_1 took values of A and 0 with equal probability. Then from (2), (3), (5), and (6) the OSNR penalty at a BER of 10^{-3} could

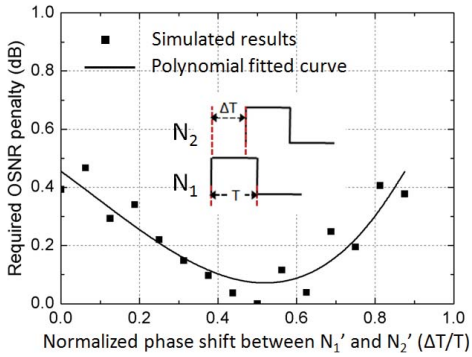

Fig. 5. Simulation results of OSNR penalty versus time misalignment between the bits of N_1 and N_2. Points are fitted with third-order polynomial.

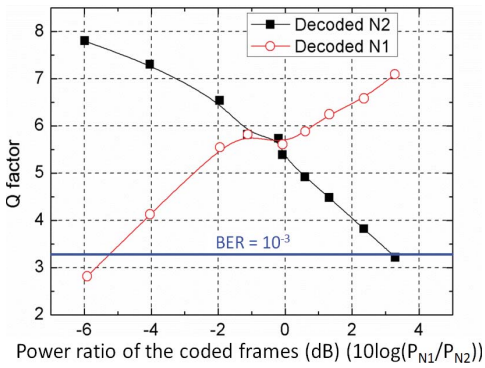

Fig. 6. Q-factors of the decoded N_1' and N_2' at different N_1, N_2 power ratios. The points are connected with spline interpolation.

be calculated and the result was 8.4 dB. Note that within the OSNR penalty 3 dB was due to the difference in the definition of OSNR for single-polarized and dual-polarized signals. The OSNR for single-polarized signal was 3 dB less than that of dual-polarized signal when the value A^2/σ^2 was the same for the two signals.

When N_1 and N_2 had the same bit rate, the dependence of the OSNR penalty on the time misalignment between the bits of N_1' and N_2' was also evaluated through simulation. As shown in Fig. 5, the variation of the OSNR penalty was less than 0.5 dB and the smallest OSNR penalty was achieved when the bit misalignment between N_1' and N_2' was half the bit interval. From (6), it could be noticed that different bit misalignment between N_1' and N_2' led to different distribution of A_1. When the bit misalignment was half the bit interval, the corresponding BER′ achieved the minimum value.

We have further studied the Q-factors when the input powers of frames N_1' and N_2' are imbalanced. In the experiment, the ASE noises in both polarizations were the same and the OSNR was 25 dB. As shown in Fig. 6, the Q-factors of the decoded N_1' and N_2' were above the forward error correction (FEC) threshold for BER $= 10^{-3}$ when the power ratio ($10\log_{10}$ (P_{N1}/P_{N2})) ranged between -6 dB to 4 dB. The wide tolerance of the power ratio variation made the proposed optical PNC scheme robust against the imbalance between the powers of the frames N_1 and N_2 before optical PNC. To achieve optimal performance of the decoded N_1' and N_2', the powers of N_1 and N_2 should be set at the same level before network coding.

In practice, the polarizations of the two multiplexed frames might not be precisely orthogonal. The required OSNR penalty induced by the loss of polarization orthogonality was simulated and shown in Fig. 7. The simulation assumed after PBC, N_1' and N_2' were linearly polarized and the angle between them was denoted by θ. The carrier phase difference between N_1' and N_2' was denoted by $\Delta\varphi$. From Fig. 7, the carrier phase difference would not affect the OSNR penalty when θ was precisely $\pi/2$. When the deviation of θ from $\pi/2$ was less than $\pm 5°$, the maximum OSNR penalty was less than 1 dB for any $\Delta\varphi$.

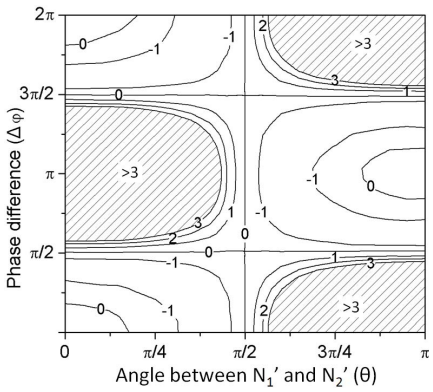

Fig. 7. OSNR penalty induced by the loss of polarization orthogonality.

VI. Summary

We have proposed and experimentally demonstrated optical PNC based on polarization multiplexing with 10-Gb/s NRZ-OOK optical frames. The proposed optical PNC scheme does not require bit synchronization and it is tolerant to power imbalance between the two input optical frames before PNC. One of the important applications of optical PNC is to effectively implement multicast protection in optical networks.

References

[1] *Cisco Visual Networking Index: Forecast and Methodology*. (2009) [Online]. Available: http://www.cisco.com/

[2] R. Ahlswede, N. Cai, S.-Y. Li, and R. W. Yeung, "Network information flow," *IEEE Trans. Inform. Theory*, vol. 46, no. 4, pp. 1204–1216, Jul. 2000.

[3] E. D. Manley, J. S. Deogun, L. Xu, and D. R. Alexander, "All-optical network coding," *J. Opt. Commun. Netw.*, vol. 2, no. 4, pp. 175–191, Apr. 2010.

[4] A. E. Kamal, "A generalized strategy for 1 + N protection," in *Proc. IEEE Int. Conf. Commun.*, May 2008, pp. 5155–5159.

[5] R. Webb, R. Manning, G. Maxwell, and A. Poustie, "40 Gb/s all-optical XOR gate based on hybrid-integrated Mach–Zehnder interferometer," *Electron. Lett.*, vol. 39, no. 1, pp. 79–81, Jan. 2003.

[6] S. Zhang, S.-C. Liew, and P. Lam, "Hot topic: Physical-layer network coding," in *Proc. 12th Annu. Int. Conf. Mobile Comput. Netw.*, Los Angeles, CA, Sep. 2006, pp. 358–365.

[7] L. Lu and S. C. Liew, "Asynchronous physical-layer network coding," *IEEE Trans. Wireless Commun.*, vol. 11, no. 2, pp. 819–831, Feb. 2012.

[8] S. Katti, S. Gollakota, and D. Katabi, "Embracing wireless interference: Analog network coding," *ACM SIGCOMM Comput. Commun. Rev.*, vol. 37, no. 4, pp. 397–408, 2007.